Indian Journal of Chemistry
Vol. 60A April 2021, pp. 489-498

Synthesis, spectroscopic characterisation, corrosion inhibition studies and dyeing properties of lanthanide(III) complexes of 1-[(3-carboxyethyl-4,5-dimethylthiophen-2-yl)azo]-2-naphthol

C J Athira[a,*], M S Sujamol[b], Y Sindhu[c] & K Mohanan[d]

[a]Department of Chemistry, MMNSS College, Kottiyam, Kollam, Kerala 691 571, India

[b]Department of Chemistry, St. Stephen`s College, Pathanapuram, Kerala 689 695, India

[c]Department of Chemistry, All Saint`s College, Thiruvananthapuram, Kerala 695 007, India

[d]Department of Chemistry, University of Kerala, Thiruvananthapuram, Kerala 695 581, India

*E-mail: aathira.ajoy@gmail.com

Received 09 September 2020; revised and accepted 15 February 2021

Ligational behaviour of the heterocyclic ligand obtained by coupling of diazotized 2-amino-3-carboxyethyl-4,5-dimethylthiophene with β-naphthol towards some selected lanthanide(III) ions has been studied. Various spectral and physico-chemical techniques have been used to confirm the coordination sites of the ligand (HTAN) and its lanthanide(III) complexes. It has been observed that these ligands coordinate to the metal ions in a neutral tridentate fashion. Thermal stability of metal chelates and structural stability of the chelating agent has been studied by thermal analysis. As lanthanides and azo dyes are reported as good corrosion inhibitors we have examined the corrosion inhibition activities of HTAN and its metal complexes. Also dyeing properties of the azo dye and some of its selected complexes towards cotton fabrics has been evaluated, as the traditional application field of the synthetic azo dyes still remains in the textile industry.

Keywords: 2-amino-3-carboxyethyl-4,5-dimethylthiophene, β-naphthol, Thermal stability, Corrosion inhibitors, Dyeing

Azo dyes are among the most profoundly explored classes of organic compounds both from theoretical and practical viewpoints. These are the largest group of organic dyes with widespread applications in many fields including dye-stuff industry, pharmacy, dosimetry, catalysis, colouring of different materials and plastics, technology of dyes and pigments, as colourants in inks due to the presence of azo (-N=N-) linkage[1]. The stability of azo compounds is boosted by the chromophoric azo group by extending the delocalised system of the arenes[2]. Owing to this well delocalised electron system, they are often brightly coloured with some of them showing orange, red and yellow colours as they absorb light having its wavelength at the visible region of the electromagnetic radiation. It is also been reported that azo dyes display good inhibitory capacity for the corrosion of several materials in both acidic and basic media[3].

A large part of the azo compounds is derived from the coupling reactions of diazotized heterocyclic amines containing aromatic hydroxy and amino group compounds. Azo compounds that contain a hydroxy group conjugated with azo-linkage can be exist in solution as an equilibrium mixture of strongly hydrogen bonded azo or hydrazone forms[4,5] and the position of equilibrium being determined by including the structure of azo compound, solvent etc. Since the tautomeric ratio is quite important parameter for the applications of dyes, investigations of the azohydrazo tautomerism are of interest both from theoretical and practical aspects[5]. Azo compounds of naphthol have been widely used as dye and they are established intermediates in the synthesis of dyes[6]. Dyes having donor atoms ortho to the azo group are well-known for their aptitude to form coordination compounds with inner metal ions[7]. The stability of the metal complexes depends upon factors with the size of the chelate rings, the basicity of ligand and the nature of metal.

In the present investigation, 2-naphthol is coupled with diazotized 2-amino-3-carboxyethyl-4,5-dimethylthiophene to form a tridentate azo derivative. The presence of electron withdrawing group such as carboxyethyl adjacent to the diazotizable amino group has a bathochromic influence on the shades of these dyes on fabric and is useful for better dispersability and dye ability[8]. Literature survey reveals[3, 9,10] that these types of dyes have been used commercially and have excellent inhibitory properties with substantial

inhibition efficiencies, and the ligational behaviour of heterocyclic ring systems and their lanthanide complexes has received comparatively less attention. This prompts us to synthesise, characterize some lanthanide(III) nitrate and chloride complexes of the title azo dye and to evaluate their dyeing properties on cotton fabric and its usage as organic corrosion inhibitor for metals in corrosive media. Apart from the synthetic, structural aspects and applications, the thermal decomposition behaviour, redox behaviour and X-ray diffraction studies are also discussed in this paper.

Materials and Methods

Chemicals

Lanthanide(III) nitrates/chlorides were prepared by treating the respective oxides by dissolvingthem in nitric acid/hydrochloric acid. The ligand, (1-[(3-carboxyethyl-4,5-dimethylthiophen-2-yl)azo]-2-naphthol) (HTAN) was prepared by the diazo-coupling of 2-amino-3-carboxyethyl-4,5-dimethylthiophene and *β*-naphthol.

Preparation of HTAN

2-Amino-3-carboxyethyl-4,5-dimethylthiophene, the starting material for the synthesis of this ligand was prepared using Gewald's elegant method[11] (Scheme 1), which provides a convenient pathway to produce stable 2-aminothiophene derivative. This was diazotized using $NaNO_2$ and concentrated H_2SO_4 at 0–5 °C. The resulting diazonium salt solution is unstable and prone to deteriorate upon standing at room temperature. The solution should always be kept at below 5 °C and should be used as soon as it is generated. The component 2-naphthol was dissolved in 10% sodium hydroxide, as it dissolves poorly in acidic aqueous solution. To prevent 2-naphthol from precipitating out prematurely, the addition of the acidic diazonium salt solution to the 2-naphthol solution should be slow (pH~8). Stir the mixture efficiently to facilitate the reaction. The product obtained was filtered off, washed with water and dried. The purity of the HTAN was checked by thin layer chromatography (TLC) (silica gel).

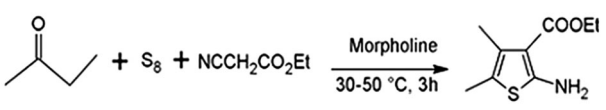

Scheme 1 — Synthesis of 2-amino-3-carboxyethyl-4,5-dimethylthiophene

Preparation of metal complexes

All the metal complexes were prepared by the following general procedure. A methanolic solution of lanthanide(III) nitrate/chloride (0.005 mol) was added to a warm magnetically stirred methanolic solution (50 mL) of the HTAN (0.01 mol). After 3 h magnetic stirring, the pH of the solution was adjusted to 6.5–7.0 and the resulting solution was then refluxed on a water-bath for about 12 h. The solution was then concentrated and kept overnight. The powdery mass separated was filtered, washed successively with MeOH and finally with ether and dried in vacuum over P_4O_{10}. The purity of the metal complexes was checked by TLC (silica gel).

Physico-chemical methods

Carbon, hydrogen, nitrogen and sulphur contents were determined by microanalysis. Molar conductance measurements were carried out with 10^{-3} M solutions of the complexes in appropriate solvents at room temperature using a Systronics direct reading digital conductivity meter Type 304. Magnetic susceptibility measurements of complexes were measured at room temperature using a Magway MSB Mk1 susceptibility balance. The measurements were made with solid specimens. The IR spectra were recorded on a Shimadzu FTIR 8201 and Perkin Elmer 817 IR spectrophotometer using KBr pellets. Far IR spectra were recorded on a Polytec FIR 30 Fourier spectrophometer using CsI discs. ^{1}H NMR spectra were recorded in DMSO–d_6, on a JEOL GSX 400NB 400MHz FT NMR spectrometer. Chemical shift of the spectra are from the signals of TMS. Electronic spectra of the HTAN and its complexes were recorded in suitable solvents in the range of 200–900 nm, using a Shimadzu 1601, UV–visible spectrophotometer. X-ray powder diffraction pattern were obtained on a Siemens D 5005 model X-ray spectrometer using Cu kα_1 radiation. Thermogravimetric analyses were carried out in dynamic air at a heating rate of 10 °C min^{-1}, using thermobalance of the type Mettler Toledo thermogravimetric system. Electrochemical behaviour of selected metal complex was studied with the help of a BAS CV-50 analyser employing glassy carbon as working electrode, Ag/AgCl as reference electrode and platinum wire as auxiliary electrode. The working media consisted of DMSO and Bu_4NPF_6 as supporting electrolyte. The solution was degassed with argon prior to use and kept under an Ar atmosphere throughout the

experiment. The measurement was carried out using 1 mM solution (DMSO) at room temperature in the potential range –1.5 to +1.5 V with a scan rate of 100 mV/sec.

Corrosion inhibition studies

Weight-loss measurements

The mild coupons were weighed and suspended vertically in aerated, unstirred 1 M H_2SO_4 (150 mL) with and without inhibitor for 15 days. After 15 days coupons were removed from solution and cleaned by brushing under running tap water to remove corrosion products, dried and reweighed to determine weight loss. The percentage inhibition efficiencies of the azo dyes and their lanthanide complexes inhibitors towards the MS in 1 M H_2SO_4 were found out from the weight loss measurements. Inhibition efficiency (%), η and a parameter surface coverage (θ) which represents the part of the surface covered by the inhibitor molecules were calculated using the following equations:

$$\text{Inhibition efficiency}, \eta = \frac{W_0 - W}{W_0} \times 100 \quad \ldots (1)$$

$$\text{Surface coverage}, \theta = \frac{W_0 - W}{W_0} \quad \ldots (2)$$

Where, W_0 and W are the weight loss in the absence and presence of the inhibitors, respectively.

Open circuit potential measurement

Open circuit potential (OCP) was measured for 15 days with 24 h interval against saturated calomel electrode using a digital multimeter. All coupons were immersed in the cell and were usually closed, but frequently opened for OCP measurements. The potential values were measured for different concentration of inhibitors without any disturbance to the strips. OCP decay of a mild steel strip kept in a blank cell *i.e*. without inhibitor was also measured to understand the extent of OCP deviation due to the presence of the inhibitor.

Dyeing procedure

Dyeing of the ligands on cotton fabric

Dyeing of the ligands on cotton fabric was carried out using a procedure reported in the literature[12]. A dispersion of the dye was produced by dissolving 2 g of dye (2% shade) in 100 mL methanol. The liquor ratio between cotton and solution was always 1:100. The dyeing process was started at 40–50 °C and the wetted-out cotton fabric was put into the dye bath. Then 2 mL of 10 % Glauber's salt solution was added followed by rising the temperature of the dye-bath to 80 °C and dyeing process was continued for 40–45 min. The dyed fabric was then rinsed with cold water and finally air dried.

Dyeing of the metal complexes on cotton fabric

The same procedure was also applied in case of metallized dyeing. The wetted-out cotton fabric was added into the dye-bath (liquor ratio = 1:100) containing 2% acetic acid. At initial stage, temperature of the dye-bath was kept at 40–50 °C meanwhile required amount of metal salt was added along with 10 % Glauber's salt solution (2 mL). The pH of the dye-bath was adjusted to 6.0–6.5 using aqueous acetic acid. Dyeing was performed by raising the dye bath temperature from 40 to 80 °C at 1.5 °/min, holding at this temperature for 45 min. The dyed fabric was then rinsed with cold water and finally dried in air.

Results and Discussion

Azo dyes containing hydroxy group conjugated to the azo group are capable of undergoing azo-hydrazone tautomerism. This type of tautomerism, which resulted from the intramolecular proton transfers between nitrogen and oxygen atoms, have been studied by various techniques. As the donor properties of the azo group are weak, the stable complexes cannot result from the donor strength of azo groups alone. A decisive factor in the formation of a chelate ring is the number of atoms involved in ring formation: chelates with five or six-membered rings are the most stable; this criterion is met by the compounds discussed here.

The observed elemental analytical data of the HTAN indicates that the diazo-coupling reaction has occurred in 1:1 ratio. The HTAN is soluble in common organic solvents and it formed well defined complexes with lanthanide(III) nitrate/chloride salts in molar ratio M: L = 1:2. Analytical data and other details of the HTAN and metal complexes are in good agreement with their formulation as given in the Supplementary Data, Tables S1 and S2.

Structure of the ligand

The structure of the HTAN has been established on the basis of elemental analysis, UV, IR and NMR spectral data.

UV-visible absorption spectrum

Absorption spectral data can be conveniently used to identify each tautomer present in the ligand under investigation. The ultraviolet spectrum of HTAN exhibited a characteristic band at 283 nm, which adequately support the existence of azo-enol form of the HTAN (Fig. 1).

Infrared spectrum

The IR spectrum of HTAN (Supplementary Data, Fig. S1) exhibited a broad band in the region 3500–3100 cm^{-1} with peak centered at 3440 cm^{-1}, attributable to the stretching vibration of naphtholic (O-H) group[13] and the naphtholic ν(C–O) stretching vibration has been observed as a medium intensity band[14] at 1271 cm^{-1}. Another medium intensity band observed at 1467 cm^{-1}, can be attributed to ν(N=N), confirming the formation of azo group in the HTAN[15]. Thus the IR spectrum strongly support the existence of the HTAN in an intramolecularly hydrogen bonded azo-enol form. Apart from these vibrations the infrared spectrum of the HTAN exhibited a prominent band at 1704 cm^{-1}, which can be assigned to the presence of ν(C=O) of the ester group[16]. The ester carbonyl group is also involved in weak hydrogen bonding with the naphtholic -OH resulting in a sort of bifunctional hydrogen bonding[17]. However, in competition with the azo group, for naphtholic -OH, ester carbonyl can manage only a little share. This elucidates why the ester carbonyl frequency in the HTAN stands relatively higher than that of the free amine at 1660 cm^{-1}. In addition to the above frequencies, vibrations characteristic of the substituted thiophene ring[18] have been observed at 1513, 1406 and 1342 cm^{-1}.

Table 1 — Magnetic and molar conductance data of $[Ln(III)(HTAN)_2(NO_3)_3]$

Complex	Magnetic moment (BM)	Molar conductance (10^{-3} M) (ohm^{-1} cm^2 mol^{-1})	
		DMF	DMSO
$[La(III)(HTAN)_2(NO_3)_3]$	Diamagnetic	12.9	7.1
$[Ce(III)(HTAN)_2(NO_3)_3]$	2.41	13.1	6.8
$[Pr(III)(HTAN)_2(NO_3)_3]$	3.53	13.4	6.3
$[Nd(III)(HTAN)_2(NO_3)_3]$	3.56	12.5	6.7
$[Sm(III)(HTAN)_2(NO_3)_3]$	1.51	12.1	6.6
$[Eu(III)(HTAN)_2(NO_3)_3]$	3.38	13.0	6.9
$[Gd(III)(HTAN)_2(NO_3)_3]$	7.82	13.5	6.1

Table 2 — Magnetic and molar conductance data of $[Ln(III)(HTAN)_2Cl_3]$

Complex	Magnetic moment (BM)	Molar conductance (10^{-3} M) (ohm^{-1} cm^2 mol^{-1})	
		DMF	DMSO
$[La(III)(HTAN)_2Cl_3]$	Diamagnetic	12.4	6.3
$[Ce(III)(HTAN)_2Cl_3]$	2.55	13.2	6.2
$[Pr(III)(HTAN)_2Cl_3]$	3.57	13.4	5.8
$[Nd(III)(HTAN)_2Cl_3]$	3.65	11.5	6.6
$[Sm(III)(HTAN)_2Cl_3]$	1.52	11.7	7.2
$[Eu(III)(HTAN)_2Cl_3]$	3.41	12.8	6.4
$[Gd(III)(HTAN)_2Cl_3]$	7.86	13.1	6.2

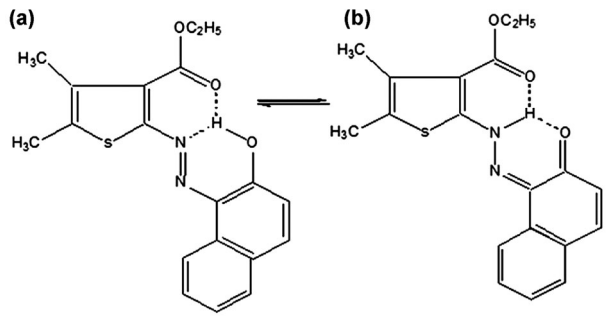

Fig. 1 — Tautomeric structure of HTAN

^{1}H NMR spectrum

The ^{1}H NMR spectrum of the HTAN (Fig. 2a) recorded in DMSO-d_6 adequately supported the conclusions drawn on the basis of UV and IR spectral data. The spectrum of the HTAN exhibited a downfield shift of the naphtholic –OH proton resonating at 15.10 δ[19]. The peaks of the hydroxyl protons are shifted downfield as a result of strong intramolecular hydrogen bonding between the diazo nitrogen and the hydroxyl proton. Signals for methyl protons and methylene protons of the ester group on the thiophene moiety have been observed at 1.45 and 4.49 δ[20], respectively. The spectrum gave clear evidence for the presence of aromatic proton signals in the range 7.25–7.80 δ[21]. Also, the signal appearing at 2.27 δ can be attributed to the two methyl groups at 4 and 5- positions on the thiophene moiety.

^{13}C NMR spectrum

The ^{13}C NMR spectrum of the HTAN (Fig. 2b) was recorded in DMSO-d_6 and the spectral data confirm the ^{1}H NMR spectral results. The signal appeared at 163.58 δ can be attributed to the presence of ester carbonyl group. The methylene and methyl group signals are appeared at 61.26 and 14.45, 14.00, 13.93 δ, respectively[22]. The signals for naphthylic carbon atoms were seen in the range of 122.03-137.66 δ[3]. The ring carbon atom attached to napththolic oxygen

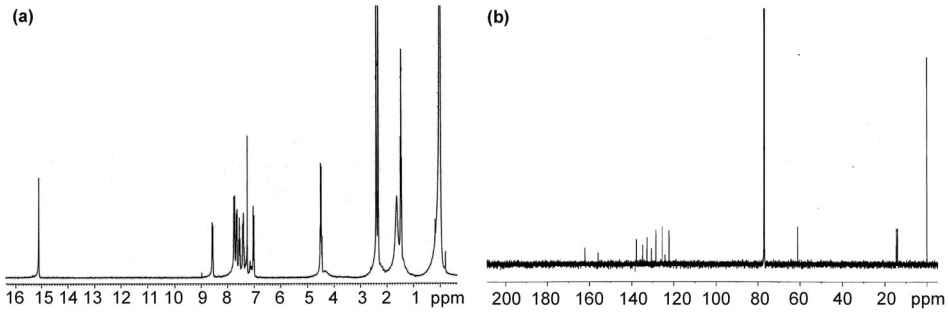

Fig. 2 — (a) ^{1}H and (b) ^{13}C NMR spectra of HTAN

atoms (C-O, aromatic) showed a downfield signal appeared at 156.03 δ[23]. This is in agreement with the azo-enol form of the HTAN. In addition to these peaks, the absence of signal of C=N of hydrazone linkage also confirms the azo-enol form. On the basis of all the above spectral data, an internally hydrogen bonded azo-enol structure has been proposed for the HTAN as shown in Fig. 1.

Structure of the metal complexes

The formulation of lanthanide(III) complexes has been made on the basis of elemental analysis, molar conductance and magnetic susceptibility measurements. The metal complexes are non-hygroscopic, light-coloured solids, decomposed above 250 °C and are soluble in DMSO and DMF. The molar conductance values in DMSO and DMF (Tables 1 and 2) reveal the non-electrolytic nature of the metal complexes[24].

The metal complexes formation can be represented by the following general equation:

$Ln(NO_3)_3 + 2HTAN \rightarrow [Ln(III)(HTAN)_2(NO_3)_3]$
$LnCl_3 + 2HTAN \rightarrow [Ln(III)(HTAN)_2Cl_3]$
where, Ln(III) = La, Ce, Pr, Nd, Sm, Eu or Gd.

IR spectra

Infrared spectral data of the metal complexes are presented in Supplementary Data Tables S3 and S4 along with their tentative assignments. In the spectra of the metal chelates (Supplementary Data, Fig. S2), the band at 1704 cm^{-1} is shifted to lower frequency by about 44 cm^{-1}, indicating coordination by the ester carbonyl. This type of coordination by ester carbonyl group has been already reported by several investigators[25]. The band due to ν(N=N), appearing at 1467 cm^{-1} in the free HTAN undergoes a negative shift by about ~25–30 cm^{-1} in the metal complexes, indicating the involvement of azo nitrogen in bonding with the metal ion[26,27]. This lowering of frequency can be explained by the transfer of electrons from the azo nitrogen atom to the metal ion due to coordination. It has been reported that the interaction of the lanthanide ion with naphtholic oxygen does not increase the acidity to be sufficient for ionization of the proton[27]. Consequently, the naphtholic oxygen is coordinated to the lanthanide ion without deprotonation. As a result of this, the band apparently due to the internally hydrogen bonded OH group is shifted to higher frequency and became less broad showing a peak centered at ~3456 cm^{-1} indicating that the hydrogen bond got weakened and oxygen atom coordinated to the metal ion without deprotonation[28]. This is further supported by a positive shift of ν(C-O) band by about 20 cm^{-1} in the metal complexes. Apart from all the above frequencies, the vibrations characteristic of the substituted thiophene ring remain almost unaffected. This observation indirectly supported the non-participation of ring sulphur atom in coordination with the metal ion.

Coordination by nitrate ion

Infrared spectral data can be successfully used for identifying the mode of bonding of nitrate group. The spectra of the nitrate complexes reveal two additional bands at 1480 cm^{-1} and 1275 cm^{-1}. These bands can be attributed to ν_5 and ν_1 modes of vibrations of the coordinated nitrate ion, respectively. The magnitude of separation between these bands (ν_5–ν_1) in the metal complexes is ~215 cm^{-1}, which indicates that the nitrate ion is coordinated to the metal ion in a bidentate fashion.

Far IR spectra

In the far IR spectra of all the metal complexes, the non-ligand bands observed at 420–425 and 360–365 cm^{-1} can be assigned to the ν(Ln–O) and ν(Ln–N) stretching vibrations, respectively. Conclusive evidence regarding the bonding of chlorine to the metal ion is provided by the

occurrence of bands at 310–315 cm^{-1} as the result of ν(Ln–Cl) mode of vibration[29]. Absence of ν(Ln–S) band gave added support to the non-participation of ring sulphur atom in coordination.

^{1}H NMR spectra

In agreement with the UV-visible and IR spectral data, the ^{1}H NMR spectra of $[La(III)(HTAN)_2(NO_3)_3]$ and $[La(III)(HTAN)_2Cl_3]$ recorded in DMSO-d_6 also exhibited signal for the OH proton at 14.98 and 15.05 δ, respectively, indicating that the OH group is coordinated to the metal ion without deprotonation. Comparison of the position of the other resonance signals in the complexes with those of the HTAN indicates downward shifting by about 0.10 to 0.20 δ in the metal complex.

^{13}C NMR spectra

The comparison of the ^{13}C NMR spectrum of the HTAN with their corresponding metal complexes reveals some useful information about the mode of bonding of compounds. In the spectrum of lanthanum(III) complex, the signals due to ester carbonyl and carbon atom attached to the naphtholic oxygen showed downward shifts by ~4.3 and 1.2 δ respectively. This observed chemical shifts may be due to the electron transfer from the carbonyl and hydroxyl oxygen atoms to La(III) ion and they confirmed the expected coordination of the HTAN. The other carbon atoms were only slightly affected from the coordination of the metal ion. Thus, from the above spectral data it is clear that the HTAN is bonded to the metal ion without deprotonation in a neutral tridentate fashion and coordination sites being naphtholic oxygen, one of the azo nitrogen atoms and ester carbonyl group. A coordination number of nine has been proposed for lanthanide(III) chloride complexes and twelve for lanthanide(III) nitrate complexes (Fig. 3). This type of higher coordination number has been already reported in literature[30].

Electronic spectra

The ultraviolet spectral bands characteristic of the azo-enol form of the ligand are marginally red shifted in the spectra of the metal complexes. It is a clear indication that no structural alteration of the ligand occurs on metal chelation. The enhancement of intensity of certain hypersensitive bands of Pr(III), Ne(III) and Sm(III) complexes compared to aquo ions can be attributed to the action of an inhomogeneous electromagnetic field and by the changes in the symmetry of the field on the lanthanide ion[31].

Magnetic properties

The magnetic moment values of the lanthanide(III) complex reveal that the lanthanum(III) complex is diamagnetic, while all others are paramagnetic and its data are tabulated in Tables 1 and 2. The measured magnetic moment of all the complexes are very close to the theoretical values calculated for the free lanthanide(III) ions except for the Sm(III) and Eu(III) complexes. This indicates that the 4*f* electrons are not much disturbed by the ligand field produced by azo dyes. The slight high value observed in the case of Sm(III) and Eu(III) complexes may presumably include temperature-dependent magnetism on account of low J-J separation[32].

X-ray diffraction study

The X-ray diffractogram of the HTAN is given in Supplementary Data, Fig. S3, has been recorded 14 reflections between 2θ ranging from 12° to 52° with maxima at 2θ = 24.9043°, which corresponds to interplanar distance d = 3.5723 Å. The main peaks have been indexed using computer software by trial-and-error method and the data obtained are presented in Supplementary Data, Table S5. The $Sin^2\theta$ and

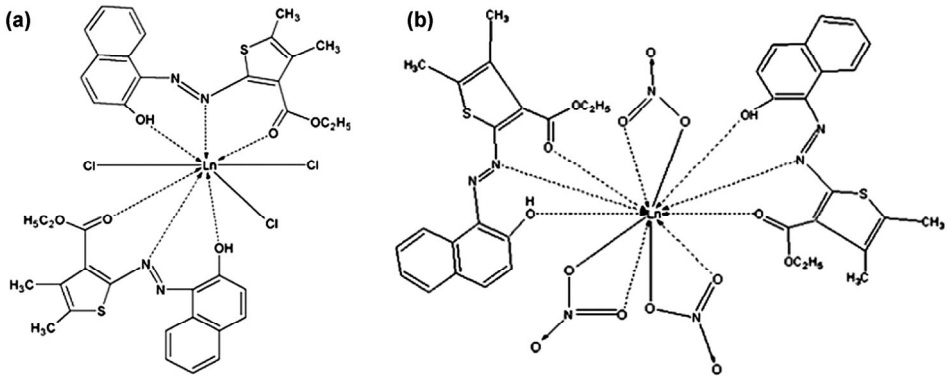

Fig. 3 — Structure of (a) $[Ln(III)(HTAN)_2Cl_3]$ and (b) $[Ln(III)(HTAN)_2(NO)_3]$

2θ values obtained have been compared with the calculated values. A comparison of these values shows good agreement between calculated and observed values. The HTAN is successfully indexed to orthorhombic crystal systems[33] with the lattice constants; a = 9.4980 Å, b = 5.0013 Å, c = 4.3938 Å and unit cell volume208.7230 $Å^3$ In order to understand the change in the state of the ligand on coordination with the metal ion, the X-ray diffraction pattern of the metal complexes have also been examined. It has been observed that the crystallinity of the ligand has been lost on complexation and became amorphous.

Cyclic voltammetry

Based on cyclic voltammogram (Fig. 4) of samarium complex, it seems likely that the reduction peak observed at –986 mV on forward scan might be attributed to the reversible reduction of the metal complex[34]. After the reversal of the scan direction the CV profile has displayed two waves at Ep_a = -618 and -378 mV. The former value is due to the reversible oxidation of the complex and the latter is due to the irreversible oxidation of the ligand; no reductive response was found[35]. The number of electrons transferred in the electrode reaction for the reversible couple can be determined from the separation between peak potential. The peak-to-peak separation (ΔEp value) obtained was 368 mV, which reveals that the redox reaction is quasi-reversible single step one electron process[36]. Also the ratio of the anodic to cathodic peak current (ip_a/ip_c) approaches 'one' at this scan rate indicating that the number of electrons transferred is 1 (n =1). From the voltammetric data, the redox process can be represented by the Eqn (3)[37].

$$Sm(III) + 1e \leftrightarrow Sm(II) \quad \ldots (3)$$

3-D molecular modeling

The molecular modeling[38] of the possible 3D structures of the HTAN and one of the metal complexes, $[La(III)(HTAN)_2Cl_3]$, as a representative, were optimized by molecular mechanics calculations, giving the lowest energy CHEM 3D models. The CHEM 3D model of the HTAN is shown in Fig. 5a, while that of $[La(III)(HTAN)_2Cl_3]$ is shown in Fig. 5b. The bond lengths and bond angles of the HTAN are given in Supplementary Data, Tables S6 and S7. Selected bond lengths and the bond angles around the lanthanum(III) ion of $[La(III)(HTAN)_2Cl_3]$ are given in Supplementary Data, Tables S8 and S9.

Thermogravimetric analysis

In order to study the thermal stability of metal complex the lanthanum(III) nitrate and chloride complexes were subjected to TG analysis . The lanthanum(III) nitrate complex (Supplementary Data, Fig. S4) decomposes in two stages, being stable up to 250 °C. At this temperature the first stage of decomposition starts and completed at 460 °C with DTG peak at 346 °C. The corresponding mass loss (28.13%) can be attributed to the loss of naphthol moiety, which agrees with the calculated mass loss of 27.70%. The second stage decomposition followed a mass loss of 68.75% (calculated mass loss, 68.48 %)

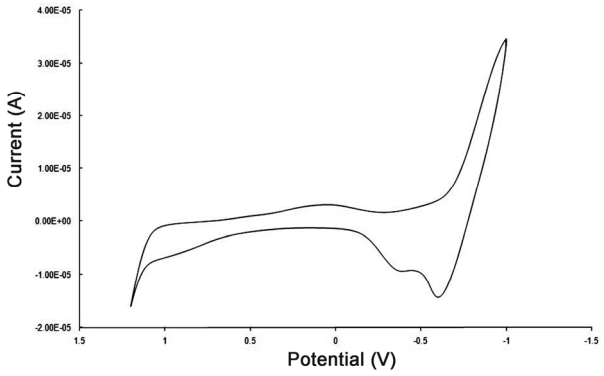

Fig. 4 — Cyclic voltammogram of $[Sm(III)(HTAN)_2Cl_3]$

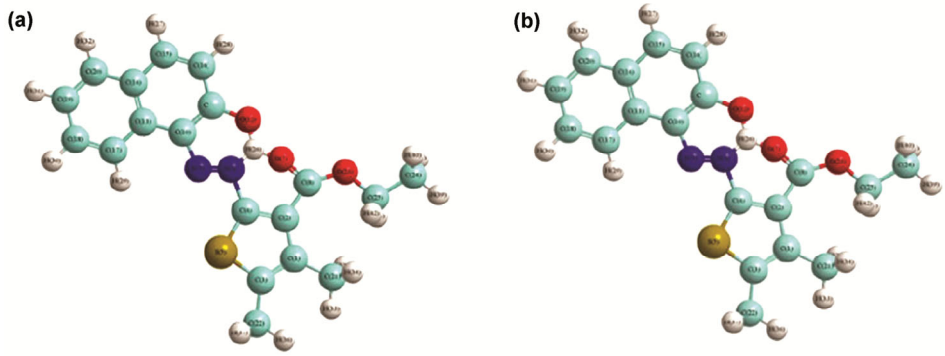

Fig. 5 — 3D molecular modeling structure of (a) HTAN and (b) $[La(III)(HTAN)_2Cl_3]$

which could be attributed to the loss of the remaining part of the ligand and oxidative decomposition of the complex to its oxide.

The lanthanum(III) chloride also shows two stage of decomposition with DTG peaks at 340 and 610 °C. The first stage of decomposition occurs in the temperature range of 260-470 °C. This can be attributed to the loss of naphthol moiety. The second stage of decomposition starts at 570 °C and become stable at 680 °C. The mass loss at this stage is due to the loss of HTAN moiety completely and the formation of La_2O_3. The mass loss agrees fairly well with the mass loss in independent pyrolysis experiments. The thermal analysis was carried up to 1000 °C and no further change was observed after 690 °C.

Corrosion inhibition activity

The organic inhibitors like azo dyes generally inhibit the corrosion process through adsorption of the inhibitor on the metal solution interface. A coordinate type of bond involving electron transfer from inhibitor to the metal is assumed to take place in this process. The effectiveness of a compound as a corrosion inhibitor depends on several factors including the structure of the compound, the number and types of adsorption sites, nature of molecule, the metal surface and the ability to form complexes. The inhibition of corrosion can be due to interactions between the lone pair of electrons present on hetero atoms and π-electron of aromatic rings, with the positively charged metal surface[39].

The corrosion inhibition activities of HTAN and $[Ce(III)(HTAN)_2Cl_3]$ were checked using weight loss method and open circuit potential measurements. The weight loss of the mild steel in the absence and presence of different concentration of ligand and metal complex was measured and compared for 15 days. It has been observed that the coupons immersed in the inhibitor solutions are corroded to a lesser extent while the coupon in the blank solution is severely corroded. The calculated values of inhibition efficiency (IE) from weight loss measurements of mild steel are listed in Table 3.

It has been found that the azo dye and its metal complex inhibit the corrosion of mild steel in 1 M H_2SO_4 at all the selected concentrations. It is also revealed from tables that the ligand and metal complex tested as inhibitor provide decrease in weight loss with increase in inhibitor concentration. Thus the inhibition efficiency increases with increase in concentration of the inhibitors. This can be attributed to an increase in the surface coverage of the inhibitor molecules on the metal surface. As concentration of additive increases it blocks the available active site on mild steel which retards dissolution of metal[3].

On comparing with the inhibition efficiency of ligand, the metal complex showed quite high inhibition efficiency. On comparing with the inhibition efficiency of ligand, the metal complex showed quite high inhibition efficiency. This can be attributed to the coordinatively unsaturated nature of lanthanides. Due to this nature, it can easily form bimetallic type complex forming protective surface films during inhibition process thus inhibiting the corrosion.

Open-circuit potential measurements

The open circuit potential (OCP) recorded for mild steel samples in 1 M H_2SO_4 with different concentrations of azo dye and metal complex at different time interval are given in Table 4. It is obvious from the result that the OCP value of blank solution is shifted towards a higher negative value which indicates severe corrosion. However, the solution containing inhibitor is able to bring the potential values towards positive region. This is due to the ability of inhibitor to form a passive film on the surface of mild steel strips thus reducing the corrosion rate. The metal complex inhibitor reduces the corrosion rate to a significant extent showing higher inhibition efficiency. The inhibition efficiency varies with the concentration of the inhibitor. As concentration of the inhibitor solution increases, the OCP value shift towards positive region. From these observations, it is clear that the concentration of inhibitor can influence the inhibition efficiency. This is in accordance with the weight loss measurements.

Table 3 — Inhibition efficiency of azo compounds using weight loss method

Inhibitor	Conc. (10^{-4} M)	Weight loss (mg/cm)	η (%)	θ
HTAN	0	0.846	-	-
	1	0.0450	46.81	0.4681
	2	0.0429	49.29	0.4929
	3	0.0415	50.94	0.5094
	4	0.0398	52.95	0.5295
	5	0.0370	56.26	0.5626
$[Ce(III)(HTAN)_2Cl_3]$	0	0.0846	-	-
	1	0.0437	48.35	0.4835
	2	0.0395	53.31	0.5331
	3	0.0374	55.79	0.5579
	4	0.0336	60.28	0.6028
	5	0.0319	62.29	0.6229

Table 4 — Variation of open circuit potential with different concentration of azo compounds

Compounds	Concentrations 10^{-4} M	Day					
		1	3	6	9	12	15
HTAN	1	-0.570	-0.562	-0.554	-0.545	-0.538	-0.524
	2	-0.565	-0.557	-0.549	-0.526	-0.514	-0.511
	3	-0.559	-0.551	-0.538	-0.521	-0.515	-0.509
	4	-0.548	-0.541	-0.529	-0.519	-0.514	-0.504
	5	-0.539	-0.533	-0.521	-0.511	-0.503	-0.487
Blank	-	-0.588	-0.598	-0.639	-0.700	-0.711	-.718
$[Ce(III)(HTAN)_2Cl_3]$	1	-0.489	-0.487	-0.474	-0.456	-0.436	-0.420
	2	-0.482	-0.476	-0.458	-0.439	-0.432	-0.417
	3	-0.479	-0.459	-0.436	-0.408	-0.398	-0.375
	4	-0.480	-0.448	-0.417	-0.397	-0.374	-0.340
	5	-0.478	-0.434	-0.390	-0.352	-0.316	-0.292

Dyeing properties

The azo dye ligand and its selected metal complexes were examined for their dyeing properties. The synthesized HTAN azodye and its Pr(III) and Nd(III) complexes were applied at 2% depth on cotton fabric, provide attractive colour with good levelness, brightness and depth on dyeing cotton fabrics. The dyeing on cotton fabric was evaluated in terms of their fastness properties using standard methods and these properties were measured using Grey Scale Rating.

The nature and position of the substituent present on the diazotized compound and coupling components has a great influence on the shade of the dyeing[40]. The heteroatoms present in the ligand structure also results in bathochromicity and leads to the brightness of shades. On dyeing the cotton fabric with metallized azo dye, it has been observed that the fabric afforded better shining shade than dyeing with ligand. This difference in colour did not find expose in the figures depicting ligand dyeing and metal complex dyeing (Fig. 6). But by evaluating the fastness properties of dyeing on cotton fabric, it has been observed that such properties have been enhanced on complexation.

It is revealed from the results shown in Table 5 that the azo dye ligand and metal complexes have fair to good fastness properties to light, washing, perspiration, rubbing and water fastness. The fastness properties of the dyeing are correlated with the structure of the dye and the substrate to which it is applied. The presence of an electron withdrawing group such as carboxyethyl adjacent to the diazotizable amino group has a bathochromic influence on the shades of these dyes on fabric and is also useful for better dispersability and dyeability.

Table 5 — Results of various fastness properties of the azo dyes and metallized azo dyes on cotton fabrics

Sample	Light fastness	Water fastness	Wash Fastness (40 °C)	Perspiration fastness		Rubbing fastness	
				Acid	Alkaline	Dry	Wet
HTAN	3	4	4-5	4	4	4	4
$[Pr(III)(HTAN)_2(NO_3)_2]$	4	5	5	5	5	5	5
$[Nd(III)(HTAN)_2(NO_3)_2]$	4	5	5	5	5	5	5

Grey scale rating: 1- very poor, 2- poor, 3- fair, 4 -good, 5- excellent

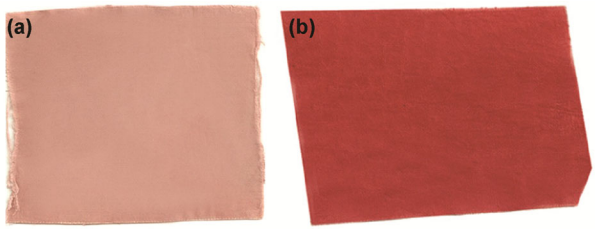

Fig. 6 — Cotton fabric dyed with (a) HTAN and (b) $[Pr(HTAN)_2NO_3]$

In this investigation slightly poorer (3-4) ratings are observed for azo dye ligand compared to the metal complexes. This can be attributed to relatively small molecular mass of azo dye and its ability to form hydrogen-bond, raising its water solubility and encouraging leaching out of the fibre. Introduction of a metal ion to the dye molecule enhances its fastness properties and the metal ion can act as an acceptor of electron donors to form coordinate bond with the dye molecule. Among the lanthanide ions Pr and Nd ions show better fastness properties. From the fastness results, it can be concluded that the rating scale having 4 & 5 of fastness properties can be magnificently used for dyeing textile fabrics, mainly on account of the facility and cheapness of the dyes synthesis, the ease of application and the overall versatility of their use.

Conclusions

The azo dye ligand obtained by the coupling of diazotised 2-amino-3-carboxyethyl-4,5-dimethylthio phene with 2-naphthol formed a series of lanthanide(III) complexes with a 1:2 metal-ligand stoichiometry. Based on the spectral data it is clear that the ligand is bonded to the metal ion without deprotonation in a neutral tridentate fashion and coordination sites being naphtholic oxygen, one of the azo nitrogen atoms and ester carbonyl group. A coordination number of nine has been proposed for lanthanide(III) chloride complexes and twelve for lanthanide(III) nitrate complexes. Earlier corrosion inhibitors such as chromates have been banned because of their high toxicity and their use produce serious environmental hazards. However, the corrosion inhibition studies showed that the azo dye reduce the corrosion rate and the inhibition efficiency is increased on complexation. It is also found that their corrosion inhibition efficiencies, increase with increase in their concentration. Thus, the azo dye ligand and their lanthanide complex can be used as an alternative in view of their low toxicity and their ecofriendly nature. Dyeing properties of azo dye ligand and its praseodymium and neodymium complexes revealed that fastness properties enhance on complexation. From the results, it can be concluded that the assessment value 4 and 5 of fastness properties can be successfully used for dyeing textile fabrics, mainly on account of the facility and cheapness of the dyes synthesis, the ease of application and the overall versatility of their use.

Supplementary Data

Supplementary Data associated with this article are available in the electronic form at http://nopr.niscair.res.in/jinfo/ijca/IJCA_60A(04)489-498_SupplData.pdf

Acknowledgement

The authors are thankful to Department of Chemistry, University of Kerala, for providing instrumental facilities.

References

1 Shams H Z, Mohareb R M, Helal M H & Mahmoud A E, *Molecules*, 16 (2011) 6271.
2 Aljamali N M, *Biochem Anal Biochem*, 4 (2015) 1.
3 Amoko J A, Aboluwoye C O & Oyeney O E, *Inter J Recent Res Appl Studies*, 6 (2019) 25.
4 Oakes J & Gratton P, *J Chem Soc Perkin Trans* 2, 9 (1998) 1857.
5 Antonov L, Kawauchi S, Satoh M & Komiyama J, *Dyes Pigm*, 38 (1998) 157.
6 Desai C K & Desai K R, *Iran Polym J*, 9 (2000) 177.
7 Snavely F A, Fernelius W C & Block B P, *J Am Chem Soc*, 79 (1957) 1028.
8 Maradiya H R & Patel V S, *Chem Heterocycl Compd*, 38 (2002) 1324.
9 Mohanan K, Athira C J, Sindhu Y & Sujamol M S, *J Rare Earths*, 27 (2009) 705.
10 Mohanan K, Aswathy R, Nitha L P, Niecy E M & Kumari B S, *J Rare Earths*, 32 (2014) 379.
11 Gewal K, Schinke E & Bottcher H, *Chem Ber*, 99 (1966) 94.
12 Czajkowski W & Szymczyk M, *Dyes Pigm*, 37 (1998) 197.
13 Omar M M & Mohamed G G, *Spectrochim Acta A*, 61 (2005) 929.
14 Thankamony M, Kumari B S, Rijulal G & Mohanan K, *J Therm Anal Calorim*, 95 (2009) 259.
15 He M, Zhou Y, Liu R, Dai J, Cui Y & Zhang T, *Dyes Pigm*, 80 (2009) 6.
16 Mohanan K & Devi S N, *Russ J Coord Chem*, 32 (2006) 600.
17 Mohanan K, *Orient J Chem*, 20 (2004) 331.
18 Rao B B, *J Vector Borne Dis*, 47 (2010) 175.
19 Tuncel M, Kahyaoglu H & Cakir M, *Transition Met Chem*, 33 (2008) 605.
20 Daniel V P, Murukan B, Kumari B S & Mohanan K, *Spectrochim Acta A*, 70 (2008) 403.
21 Yen M S &Wang I J, *Dyes Pigm*, 62 (2004) 173.
22 Abd-El-Aziz A S & Afifi T H, *Dyes Pigm*, 70 (2006) 8.
23 Saydam S, *Synth React Inorg Met-Org Chem*, 32 (2002) 437.
24 Geary W J, *Coord Chem Rev*, 7 (1971) 81.
25 Mohanan K & Devi S N, *Synth React Inorg Met-Org Chem*, 36 (2006) 441.
26 Thankamony M & Mohanan K, *Indian J Chem*, 46A (2007) 247.
27 De Sa G F, Giesbrecht E & Thompson L C, *J Inorg Nucl Chem,* 37 (1975) 109.
28 Mohanan K & Devi S N, *Synth React Inorg Met-Org Chem*, 36 (2006) 441.
29 Cotton S A, *C R Chimie*, 8 (2005) 129.
30 Paschalidis D G, *Synth React Inorg Met-Org Chem*, 34 (2004) 1401.
31 Karraker D G, *Inorg Chem*, 6 (1967) 1863.
32 Rao T R & Singh G, *Synth React Inorg Met-Org Chem*, 19 (1989) 263.
33 D'Eye R W M & Wait E, *X-ray Powder Photography in Inorganic Chemistry*, (Butterworths, London) 1960, p. 222.
34 Daniel V P, Murukan, B, Kumari B S & Mohanan K, *Spectrochim. Acta A*, 70 (2008) 403.
35 Murukan B, Kumari B S & Mohanan K, *J Coord Chem*, 60 (2007) 1607.
36 Mahalingam V, Karvembu R, Chinnusamy V & Natarajan K, *Spectrochim Acta A*, 64 (2006) 886.
37 Kuznetsov S A, Gaune-Escard M, *J. Nucl. Mater*, 389 (2009) 108.
38 Nair M L H & Thankamani D, *J Serb Chem Soc*, 76 (2011) 221.
39 Maradiya H R & Patel V S, *J Serb Chem Soc*, 67 (2002) 17.
40 Gordon P F & Gregory P, *Organic Chemistry in Colour*, (Springer-Verlag, New York) 1983, p.95.